

Controlled growth of Co nanoparticle assembly on nanostructured template $\text{Al}_2\text{O}_3/\text{NiAl}(100)$

Wen-Chin Lin

Department of Physics, National Taiwan University, 10617 Taipei, Taiwan and Institute of Atomic and Molecular Sciences, Academia Sinica, 10617 Taipei, Taiwan

Shen-Shing Wong, Po-Chun Huang, Chii-Bin Wu, Bin-Rui Xu, Cheng-Tien Chiang, and Hong-Yu Yen

Department of Physics, National Taiwan University, 10617 Taipei, Taiwan

Minn-Tsong Lin^{a)}

Department of Physics, National Taiwan University, 10617 Taipei, Taiwan and Institute of Atomic and Molecular Sciences, Academia Sinica, 10617 Taipei, Taiwan

(Received 18 May 2006; accepted 16 August 2006; published online 10 October 2006)

Based on the systematic studies of the growth temperature, deposition rate, and annealing effects, the control of Co nanoparticle density, size, and alignment is demonstrated to be feasible on a nanostructured template $\text{Al}_2\text{O}_3/\text{NiAl}(100)$. At 140–170 K, a slow deposition rate (0.027 ML/min) promises both the linear alignment and the high particle density. 1.5 ML Co nanoparticle assembly sustains the density of $\sim 260/10^4 \text{ nm}^2$ even after 800–1090 K annealing. This study also indicates the possibilities of the controlled growth for nanoparticles of different materials. © 2006 American Institute of Physics. [DOI: 10.1063/1.2358926]

Due to the potential applications in electronic and magnetic nanodevices as well as for catalysts in growing further various nanomaterials such as nanotubes or nanowires, many methods are developed in recent years for the fabrication of nanoparticle assembly. Because of the high cost and resolution limit of conventional lithography, self-organized approach of growing metallic materials on insulating substrates has been realized to be a promising way for growing nanodots with uniform size. ^{1–12} As reported in previous studies, ^{6–8,13} the single-crystalline Al_2O_3 layer grown on NiAl(100) through high temperature oxidation provides a superior template for the nanoparticle assembly. Co nanoparticles can be prepared by thermal deposition on the single-crystalline $\text{Al}_2\text{O}_3/\text{NiAl}(100)$ with such features as uniform size distribution, well-ordered alignment (interdistance $\sim 4 \text{ nm}$), and high thermal stability. Since the nanoparticles are self-organized, it is interesting to ask if there are any possibilities to control the growth of nanoparticles for the various intentions. For example, high particle density with proper particle size might be useful for catalyzing the oxidation of carbon monoxide. ³ High particle density with good alignment might lead to the formation of nanowires, which are expected to reveal the electronic and magnetic properties different from bulk and thin film materials. In this letter, we take Co as an exemplification to study the various effects of growth temperature, deposited coverage, deposition rate, and thermal annealing. Since not only Co but also Fe, Cu, etc., have been shown to reveal the similar growth mode in the particle size and alignment, on the $\text{Al}_2\text{O}_3/\text{NiAl}(100)$, ⁶ the detailed understanding of the controlled growth of Co nanoparticles in this letter might be a good example for other nanoparticle assembly composed of different materials in the further research and application.

The experimental apparatus and the preparation of $\text{Al}_2\text{O}_3/\text{NiAl}(100)$ template are described in our previous

report. ⁶ Since the deposition rates were calibrated from the epitaxial growth on Cu(100), ⁷ 1 ML was defined as the atom density on Cu(100) surface: $1.54 \times 10^{15} \text{ at./cm}^2$. Due to the limitation of instruments, the sample is prepared in a preparation chamber connected to scanning tunneling microscope (STM) chamber. Thus it is unavoidable to recover the room temperature (RT) during the sample transportation. The morphology of the nanoparticle assembly was investigated by STM at RT, with the bias voltage of 1.6–2.0 V and the tunneling current of 0.8–1.0 nA.

Figures 1(a) and 1(b) exhibit the STM images of 0.08

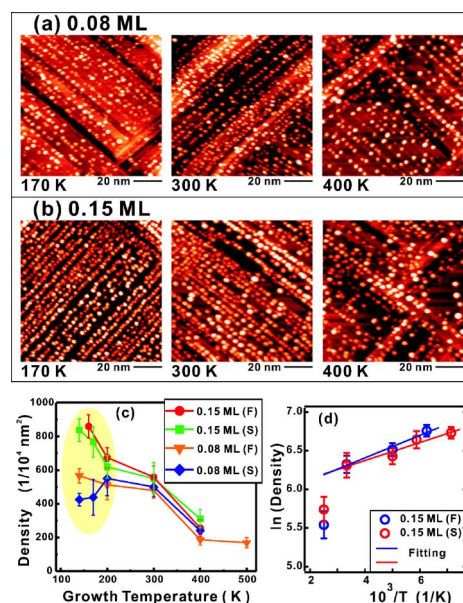


FIG. 1. (Color online) (a) and (b) are STM images of 0.08 and 0.15 ML Co on $\text{Al}_2\text{O}_3/\text{NiAl}(100)$ grown at various temperatures with the deposition rate=0.027 ML/min. (c) The statistics of nanoparticle density as functions of growth temperature (T_G) with different coverages and deposition rates. (F) and (S) denote the fast and low deposition rates of 0.27 and 0.027 ML/min, respectively. (d) Logarithm of 0.15 ML Co particle density as a function of $10^3/T$ with the Arrhenius fitting lines.

^{a)}Electronic mail: mtlin@phys.ntu.edu.tw

and 0.15 ML Co nanoparticles at different growth temperatures (T_G) (deposition rate=0.027 ML/min). Figure 1(c) summarizes the statistics of particle density as functions of T_G with different coverages (0.08 and 0.15 ML) and different deposition rates (0.27 and 0.027 ML/min). For 300–400 K growth, the statistics of the four different growth conditions are very similar. When ≤ 200 K, the curves can be separated into two groups: 0.15 and 0.08 ML Co. For 0.15 ML Co, the deposition rate effect is shown to be minor and the particle density increases monotonically with reducing T_G . But for 0.08 ML Co, the particle density is nearly invariant with reducing T_G . In general, the mobility of nanoparticles strongly depends on their sizes. The small ones can move more easily than large ones due to the less binding to the substrate. Therefore high T_G , which means high thermal energy, might activate small particles moving more easily than low T_G , resulting in the reduce of particle density. Thus intuitively, the particle density should decrease monotonically with increasing T_G , as the case of 0.15 ML Co. Apparently 0.08 ML Co does not follow the expected trend. The reason might be that even the high particle density can be prepared at low T_G , warming up to RT will trigger the diffusion of the small particles to form large ones. The 0.15 ML deposition at low T_G provides more Co atoms to enlarge and stabilize the particles with high density, so that the high density at low T_G survives after warming up to RT for 0.15 ML deposition and routs for 0.08 ML.

For the case of irreversible nucleation, both the mean field theory and Monte Carlo studies predict the particle density N to be of the Arrhenius form.^{14,15} $N \propto \exp(E_m/kT)$, where E_m is the activation energy. The proportional factor is a function of the coverage, deposition rate, and diffusion coefficient. The Arrhenius form of N can be extended for two-dimensional and three-dimensional island growths, with different proportional factors.^{14,15} In Fig. 1(d), for 0.15 ML Co, the particle density between 300–140 K indeed follows the Arrhenius form. There exists a transition between 300 and 400 K [Fig. 1(d)]. Similar phenomena are also reported in other systems.^{14–16} It is usually attributed to the transition between different growth mechanisms, for example, from the single atom diffusion to the moving and coalescence of small particles.¹⁶ From the fitting in Fig. 1(d), E_m is deduced to be 10.1 ± 1.8 and 12.9 ± 2.0 meV for the slow (0.027 ML/s) and fast (0.27 ML/s) deposition rates, respectively. The $E_m \sim 10$ meV is quite small as compared to the studies of metal islands on metal,^{14–16} in which $E_m \sim 1–0.4$ eV. Nevertheless, similar results of low E_m are reported in the studies of metal on oxide^{17–19} or nanostructured surface.²⁰ There are two common features in these studies, as well as in this work. (1) The E_m is relatively small as compared with metal on metal. It also means that the particle density is weakly affected within one order of magnitude as T_G is changed between 300 and 100 K.^{17–20} In the cases of metal on metal, particle density N can be easily enhanced by one to two orders of magnitude when T_G varies from 100 to 300 K.^{14–16} (2) The island density depends weakly on the deposition rate when $T_G < 300–400$ K. In the previous studies of Cu/TiO₂,¹⁷ Au/armorphous Al₂O₃,¹⁸ as well as this work, for an order of magnitude increase in deposition rate, the island density increases by $< 10\%$. In the studies of metal/oxide^{17–20} or nanostructured surface,²⁰ the surface defects are shown to play an important role in the adatom diffusion and particle density. For the single-crystalline Al₂O₃/NiAl(100), the periodical

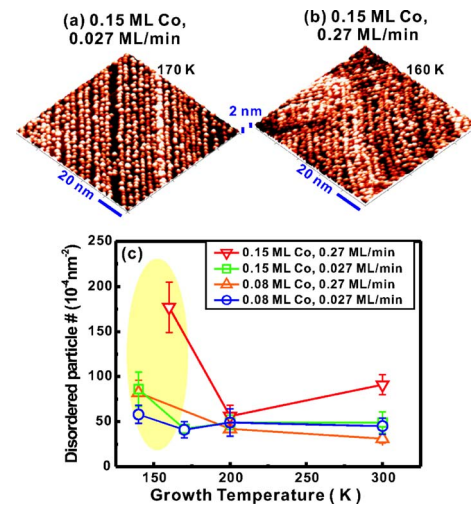


FIG. 2. (Color online) (a) and (b) are STM images of 0.15 ML Co/Al₂O₃/NiAl(100) prepared with different deposition rates at 170 and 160 K, respectively. (c) The statistics of disordered particle density as functions of growth temperature.

stripes with the interdistance ≈ 4 nm, which reveal significant attraction for Co atoms, can also confine the diffusion of adatoms or small particles. It prevents or delays the very low particle density with increasing T_G .

Although in Fig. 1 the deposition rate reveals very minor effects on the particle density than coverage, it is shown to play a critical role in the linear alignment of nanoparticles in Fig. 2. For 0.15 ML Co deposited with a slow deposition rate (0.027 ML/min) at 170 K, the nanoparticles are well aligned, following the stripes of the Al₂O₃/NiAl(100) template. In contrast, a fast deposition rate (0.27 ML/min) results in disorder of the particle alignment. Although the same amount of Co atoms (0.15 ML) is deposited, the disorder of particle alignment, higher particle density, as well as the enlarging effect from STM tip make Fig. 2(b) seems to have higher Co coverage than Fig. 2(a), which is actually not true. At lower T_G , the diffusion rate of deposited atoms is slower. Thus the deposited atoms might meet each other and create nucleations before arriving the Al₂O₃ stripes, incurring disorder of particle arrangement, while a slow deposition rate prevents the deposited atoms from creating nucleations before arriving the stripes of oxide layer. Figure 2(c) summarizes the density of disordered particles as functions of T_G . The “disordered particles” here are defined as the nanoparticles which are not aligned by the Al₂O₃ stripes. Apparently 0.15 ML Co deposited at 160 K with 0.27 ML/min reveals more disorder than that grown at 140–170 K with 0.027 ML/min. However, there are no observable differences for 0.08 ML Co grown at 140–170 K with different deposition rates [Fig. 2(c)]. As mentioned in the discussion of Fig. 1, 0.08 ML is not enough to stabilize the nanoparticles during warming up to RT. In other words, small particles in 0.08 ML Co grown at 140–170 K are capable of moving toward the oxide stripes while warming to RT. Thus no observable difference exists for low temperature (LT)-grown 0.08 ML Co with different deposition rates.

Figures 3(a) and 3(b) show the STM images of 0.15 and 1.5 ML Co nanoparticle assemblies grown at RT (deposition rate=0.5 ML/min) after annealing at various temperatures for 30 min. Figure 3(c) summarizes the statistics of particle density as a function of annealing temperature. For 0.15 ML

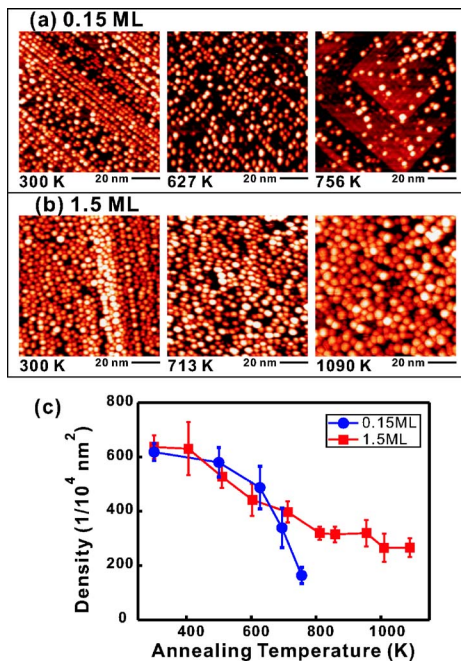


FIG. 3. (Color online) STM images of (a) 0.15 and (b) 1.5 ML Co after grown at 300 K and annealed at different temperatures. (c) Summary of the particle density as functions of annealing temperature.

Co, 627 K annealing induces the diffusion along the stripes, resulting in particle sintering and reducing the density to 80%, without losing the alignment [middle image in Fig. 3(a)]. After 695 and 756 K annealing, the density significantly drops to only 26%. For 1.5 ML, the density gradually reduces to 50% during annealing at 400–800 K. For further annealing at 800–1090 K, the particle density sustains nearly the same value: ($\sim 300\text{--}260$)/(10^4 nm^2), about 50%–40% of the as-grown density. From Fig. 3(b), the particle size is apparently enlarged due to the sintering of smaller particles, but the width of size distribution does not spread out. Even after 1090 K annealing, no particles of very large size ($> \sim 6\text{--}8 \text{ nm}$ in diameter) can be observed. It also suggests that such size of supported Co nanoparticles on $\text{Al}_2\text{O}_3/\text{NiAl}(100)$ should be stable up to as high as 1090 K.

With the understanding of the growth temperature, deposition rate, and thermal annealing effects, the controlled growth of Co nanoparticles can be demonstrated, as shown in Fig. 4. The particle density is analyzed in each process as a function of total coverage. At first, 0.15 ML Co particles are prepared at 170 K with low deposition rate (0.027 ML/min), revealing high density and well alignment in Fig. 4(a). Afterward 0.08 ML Co is deposited at 300 K with low deposition rate for three times. Based on the idea discussed in the section of growth-temperature effect, growth at higher temperature with low deposition rate promises the deposited atoms to arrive the nucleations, which is already prepared in advance, without meeting other atoms. Thus the nanoparticles in Fig. 4(b) can be enlarged without change of density. Statistical analysis in Fig. 4(a) indicates that the particle density is kept at $\sim 800/(10^4 \text{ nm}^2)$ with the total coverage up to 0.39 ML. After 0.39 ML, the nanoparticle assembly is annealed at 500 K for 30 min, resulting in notable reduce of density. Sequential Co deposition at RT also enlarges the particle size both in height and diameter with the density kept at $\sim 600/(10^4 \text{ nm}^2)$. Figure 4 reveals thus a procedure of controlled growth for Co nanoparticles.

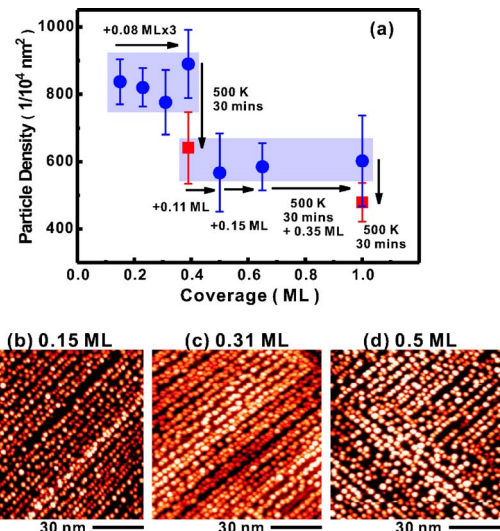


FIG. 4. (Color online) (a) Sequential particle density with variation of deposited coverage. (b)–(e) are STM images with different total coverages during the processes exhibited in (a).

In summary, a slow deposition rate (0.027 ML/min) at LT promises the good linear alignment and high particle density. Relative to 0.15 ML Co, 1.5 ML Co nanoparticle assembly reveals the high thermal stability of sustaining the density $\sim 260/(10^4 \text{ nm}^2)$ after 800–1090 K annealing. The detailed understanding of the controlled growth of Co nanoparticle might be a good exemplification for other nanoparticle assembly composed of different materials.

This work was supported by the National Science Council of Taiwan under Grant Nos. NSC 94-2112-M-002-005, 95-2120-M-002-015, and 95-2112-M-002-MY3.

- ¹J. P. Pierce, M. A. Torija, Z. Gai, Junren Shi, T. C. Schulthess, G. A. Farnan, J. F. Wendelken, E. W. Plummer, and J. Shen, *Phys. Rev. Lett.* **92**, 237201 (2004).
- ²Z. Gai, B. Wu, J. P. Pierce, G. A. Farnan, D. Shu, M. Wang, Z. Zhang, and J. Shen, *Phys. Rev. Lett.* **89**, 235502 (2002).
- ³M. Valden, X. Lai, and D. W. Goodman, *Science* **281**, 1647 (1998).
- ⁴S. Gwo, C.-P. Chou, C.-L. Wu, Y.-J. Ye, S.-J. Tsai, W.-C. Lin, and M.-T. Lin, *Phys. Rev. Lett.* **90**, 185506 (2003).
- ⁵H.-J. Freund, *Surf. Sci.* **500**, 271 (2002).
- ⁶W. C. Lin, C. C. Kuo, M.-F. Luo, Ker-Jar Song, and Minn-Tsong Lin, *Appl. Phys. Lett.* **86**, 043105 (2005).
- ⁷W. C. Lin, P. C. Huang, Ker-Jar Song, and Minn-Tsong Lin, *Appl. Phys. Lett.* **88**, 153117 (2006).
- ⁸M. F. Luo, C. I. Chiang, H. W. Shiu, S. D. Sartale, and C. C. Kuo, *Nanotechnology* **17**, 360 (2006).
- ⁹M. Bäumer, M. Frank, M. Heemeier, R. Kühnemuth, S. Stempel, and H.-J. Freund, *Surf. Sci.* **454–456**, 957 (2000).
- ¹⁰M. Heemeier, S. Stempel, Sh. K. Shaikhutdinov, J. Libuda, M. Bäumer, R. J. Oldman, S. D. Jackson, and H.-J. Freund, *Surf. Sci.* **523**, 103 (2003).
- ¹¹W. Chen, K. P. Loh, H. Xu, and A. T. S. Wee, *Langmuir* **20**, 10779 (2004).
- ¹²W. Chen, K. P. Loh, H. Xu, and A. T. S. Wee, *Appl. Phys. Lett.* **84**, 281 (2004).
- ¹³M. F. Luo, C. I. Chiang, H. W. Shiu, S. D. Sartale, T. Y. Wang, P. L. Chen, C. C. Kuo, *J. Chem. Phys.* **124**, 164709 (2006).
- ¹⁴Harald Brune, *Surf. Sci. Rep.* **31**, 121 (1998).
- ¹⁵J. A. Venables, G. D. T. Spiller, and M. Hanbücken, *Rep. Prog. Phys.* **47**, 399 (1984).
- ¹⁶A. Steltenpohl and N. Memmel, *Surf. Sci.* **454–456**, 558 (2000).
- ¹⁷J. Zhou and D. A. Chen, *Surf. Sci.* **527**, 183 (2003).
- ¹⁸J. Carrey, J.-L. Maurice, F. Petroff, and A. Vaurès, *Phys. Rev. Lett.* **86**, 4600 (2001).
- ¹⁹G. Hass, A. Menck, H. Brune, J. V. Barth, J. A. Venables, and K. Kern, *Phys. Rev. B* **61**, 11105 (2000).
- ²⁰B. Fischer, H. Brune, J. V. Barth, A. Fricke, and K. Kern, *Phys. Rev. Lett.* **82**, 1732 (1999).